

N. Bunjes
S. Paul
J. Habicht
O. Prucker
J. R uhe
W. Knoll

On the swelling behavior of linear end-grafted polystyrene in methanol/toluene mixtures

Received: 4 March 2004
Accepted: 7 April 2004
Published online: 30 April 2004
© Springer-Verlag 2004

N. Bunjes · S. Paul · J. Habicht
O. Prucker · J. R uhe · W. Knoll (✉)
Max-Planck-Institut f ur Polymerforschung,
Ackermannweg 10,
55128 Mainz, Germany
E-mail: knoll@mpip-mainz.mpg.de

Abstract Neutron reflectivity measurements have been performed with polystyrene (PS) brushes of different graft densities σ ranging from $\sigma = 0.020$ to $\sigma = 0.051$ in contact with toluene/methanol mixtures of different composition. The brushes were prepared by a “grafting-from” procedure resulting in linear chains of average molecular weight $M_n = 300,000 \text{ g mol}^{-1}$. The recorded reflectivity curves could be analyzed to a first approximation by assuming a flat scattering length density profile within the brush normal to the surface with a moderate Gaussian

smearing of the interface brush/solvent. With increasing toluene content a substantial thickness increase was found with the swollen brush at 70 vol.% being 3.7 times thicker than the dry collapsed film. At low toluene contents the preferential incorporation of this good solvent for the PS brush exceeds a factor 3.5 relative to the molar ratio of the bulk solvent mixture with methanol.

Keywords Swelling behavior · Linear end-grafted polystyrene · Methanol · Toluene · Polystyrene

End-grafted polymers (“tethered polymers” or “polymer brushes”) are interesting systems for a number of practical reasons originating from their use as lubricants, in colloidal stabilization, or as compatibilizers [1]. From a fundamental polymer science point of view they exhibit numerous interesting structural and dynamical features depending, e.g., on chain length and graft density, as well as on chain-chain, chain-substrate and, in particular, chain-solvent interactions [2]. All these factors determine how chains that are forced to overlap by a high graft density avoid crowding by stretching normal to the grafting sites, thereby balancing the interaction energy per chain and the elastic free energy. The interplay of these two terms determines the equilibrium (swelling) behavior of grafted chains [3]. The theoretical treatment of the problem started with the Alexander model [4] and the scaling predictions by de Gennes [5]. Recently, analytical self-consistent field theories [6, 7, 8] as well as Monte Carlo and molecular dynamics simu-

lations were put forward in order to describe the density profile of polymer brushes in the different regimes of graft density and solvent quality [9, 10, 11], as well as the brush behavior under shear [12].

Experimentally, the situation is somewhat complex in that early attempts to verify the theoretical predictions were carried out with brushes the endgroups of which were only physisorbed to the solid substrate [13, 14, 15, 16]. In these experiments the chains needed to remain in contact with the polymer solution. Therefore, the graft density was determined by the balance between the grafting group/ substrate interaction and the osmotic pressure that stretched the chain and, hence, was dependent on solvent quality, temperature, etc. Moreover, after desorption the individual coil in the strongly overlapping regime might have been heavily entangled and, therefore, the polymer brush was actually a mixture of grafted and trapped chains. Attempts to overcome these problems by chemically grafting the chains to the

support [17, 18, 19] resulted in the typical limitations of this preparation scheme, i.e., in a moderate graft density and/or relatively low chain lengths only. Even though some evidence for the formation of a brush was revealed by neutron reflectometry measurements, the accessible range of graft densities and chain lengths remains rather small [20]. This fundamental problem of the “grafting-to” process had led de Gennes already 1980 to propose that “rather than bringing polymer chains to the surface and attaching them there, it may be preferable to synthesize them in situ, from an initiator site on the surface” [5].

This is exactly our approach for the preparation of high molecular weight/high graft density brushes used in the present study. The synthetic route is summarized in Fig. 1[21]. A monofunctional silane derivative of azoisobutyronitrile (AIBN) as a radical initiator is coupled to the SiO_x -surface of a flat Si wafer in a self-assembly process. After activation by heat or light in the presence of a suitable monomer solution a polymer monolayer can be grown, composed of chains whose degree of polymerization and graft site density can be controlled over wide ranges and independently from each other by the proper choice of solvent, temperature, addition of free AIBN initiator in solution, length of the polymerization process, etc. Thus, a wide range from very dilute to highly crowded regimes, characterized by the aspect ratio L/D , with L being the average layer thickness and D the mean chain separation distance, can be covered. For the more interesting high density side it was shown that polymers with molecular masses exceeding 10^6 g/mol at chain distances $D \approx 2$ nm can be grown [21]. For the neutron reflectivity (NR) measurements discussed here, we prepared polystyrene (PS) brushes of $M_n = 300,000$ g/mol at three different chain separation distances $D_1 = 3.0$ nm, $D_2 = 3.8$ nm, and $D_3 = 4.7$ nm, respectively. Assuming a statistical segment size for PS of $a = 0.67$ nm [18] we obtain graft densities $\sigma = (a/D)^2$ of $\sigma_1 = 0.051$, $\sigma_2 = 0.031$, and $\sigma_3 = 0.020$, respectively.

For the X-ray and neutron reflectometry (NR) measurements we used as substrates polished silicon single crystals ($100 \times 50 \times 10$) mm³ which were cleaned at least four times for 15 min with 30% aqueous hydrogen peroxide and concentrated sulfuric acid (95%) in a 1:4 mixture (“piranha”)¹, thoroughly rinsed with deionised water and dried in air prior to modification. The synthesis of the initiator, the immobilization, and the polymerization are described in detail elsewhere [21]. Briefly, the initiator is immobilized from dried and distilled toluene. Dried triethylamine is added as base. The reaction is carried out under inert gas conditions at room temperature for at least 15 h. The polymerizations

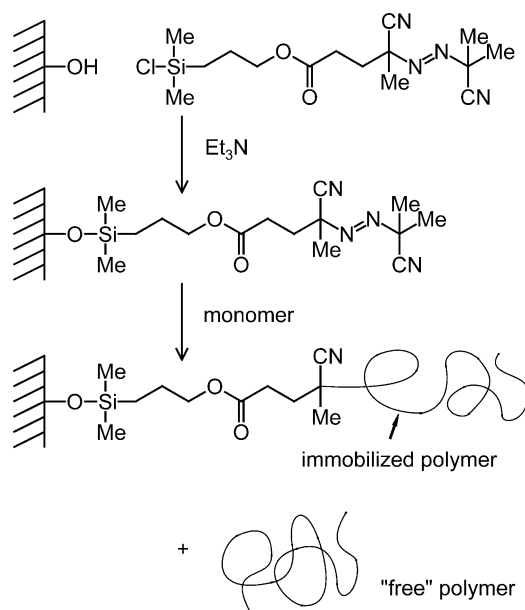


Fig. 1 Reaction scheme for the preparation of polymer brushes by the “grafting-from” technique: an initiator analog is self-assembled via its chlorosilane functionality to a solid substrate exposing OH groups. Activation of the initiator (by heat or light) leads to the formation of two radicals (one surface-bound, the other one free in solution) which—in the presence of suitable monomers—start the growth of two polymer chains, one immobilized, the other free

were performed in toluene/styrene mixtures (1/1, v/v) at 60 °C. The styrene was dried and distilled prior to use and the solutions were carefully degassed during at least three freeze-thaw cycles to remove residual oxygen. In the case of the samples described below, the polymerization time were 6, 7, and 9 h, respectively. After polymerization each sample was extracted with hot toluene in a Soxhlet apparatus for at least 15 h to remove all physisorbed polystyrene from the sample. The samples were dried in air and the dry thicknesses determined by X-ray reflectometry (XR) and by NR.

X-ray data were taken prior to the swelling experiments. The X-ray reflectometer used [22] utilizes an 18-kW rotating anode with a copper target, a graphite monochromator, and a scintillation counter. The CuK_α radiation at a wavelength of 0.1514 nm was used. The data analysis using a matrix technique is described elsewhere [23, 24].

Neutron reflectivity data were taken at the reflectometer TOREMA II [25] at the GKSS in Geesthacht. The wavelength was fixed to 0.43 nm by a graphite monochromator. A position sensitive He^3 detector allows for a resolution of $\Delta\theta = 0.005^\circ$. The incidence angle was varied typically in steps of 0.01° over a maximum range from $\theta = 0.1^\circ$ to $\theta = 1.2^\circ$ covering the critical angle for total internal reflection as well as the range of higher incident angles which reveals details on the polymer solvent interface.

¹WARNING: piranha may react explosively with organic material.

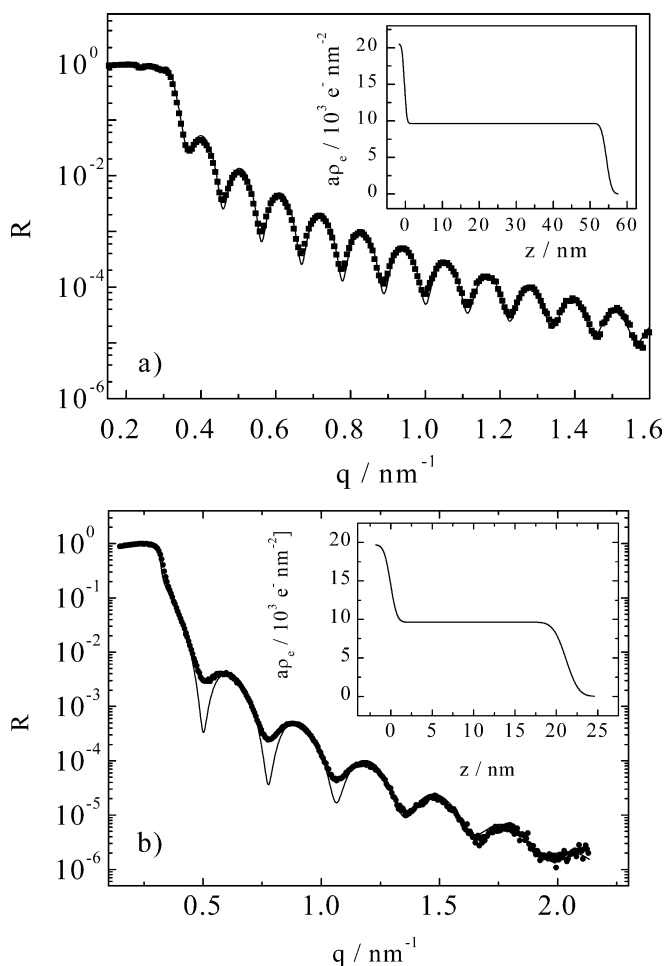


Fig. 2a,b X-ray reflectivity curves, i.e., reflectivity R vs momentum transfer q , for two dry, collapsed polystyrene brushes with a thickness of: **a** $d_0 = 53$ nm; **b** $d_0 = 19.5$ nm. Symbols are the data points, full curves are Fresnel fits based on the electron density profile ρ_e (amplified by the electron radius a) given in the respective insets

During the NR scans the samples were kept in contact with perdeuterated methanol/toluene mixtures $[(d - \text{MeOH})_1 - x_0 / (d - \text{toluene})_{x_0}]$ of different volume fractions x_0 of toluene. For contrast variation experiments mixtures of protonated and perdeuterated methanol and toluene solvents were used.

Prior to the NR scans XR measurements were performed with the polymer layers being in a collapsed dry

state in air. Figure 2 shows for two different samples the obtained R -vs- q curves together with the Fresnel simulations based on electron density profiles given in the respective insets. A three layer model, Si/PS/air, with roughness parameters $\Delta\sigma$ (describing the width in the errorfunction used to model the interface) for the Si/PS interface, $\Delta\sigma_1$, and for the PS/air interface, $\Delta\sigma_2$, respectively, was sufficient to describe the experimental data. The remarkable flatness of the layer surface was further confirmed by AFM images that revealed a typical roughness of less than 1.2 nm. The obtained dry layer thicknesses, the interfacial roughness parameters and the electron densities are summarized in Table 1.

Figure 3 displays a series of NR scans taken from the same two PS-brushes, but in contact with different $d - \text{MeOH}_1 - x_0 - \text{toluene}_{x_0}$ solvent mixtures as indicated. The symbols are the data points, the full curves again Fresnel simulations based on the scattering length density profiles given in Fig. 4. For all samples, Si was modeled with a scattering length density of $\frac{b}{V}|_{\text{Si}} = 2,07 \times 10^{-4} \text{ nm}^{-2}$. Other than in the X-ray case where the electron density of SiO_2 is almost identical to that of Si and hence the oxide layer of the Si wafer can be ignored in the Fresnel fits, we introduced for the NR simulation a 2.5 nm thick native SiO_2 layer with a scattering length density of $\frac{b}{V}|_{\text{SiO}_2} = 3,4 \times 10^{-4} \text{ nm}^{-2}$. The roughnesses of the Si/ SiO_2 and SiO_2 /PS interfaces were both assumed to be 0.6 nm. Figure 3a displays the series of NR data obtained with the thicker sample ($d_0 = 55$ nm) focusing on solvent mixtures with a low to moderate toluene content. The data shown in Fig. 3b were taken with the thinner sample ($d_0 = 19.5$ nm) extending the toluene content of the solvent mixtures to higher fractions. In addition a NR scan taken in air is displayed for comparison (with the data recorded in MeOH as well as taken by X-ray reflectometry, cf. Fig. 2b).

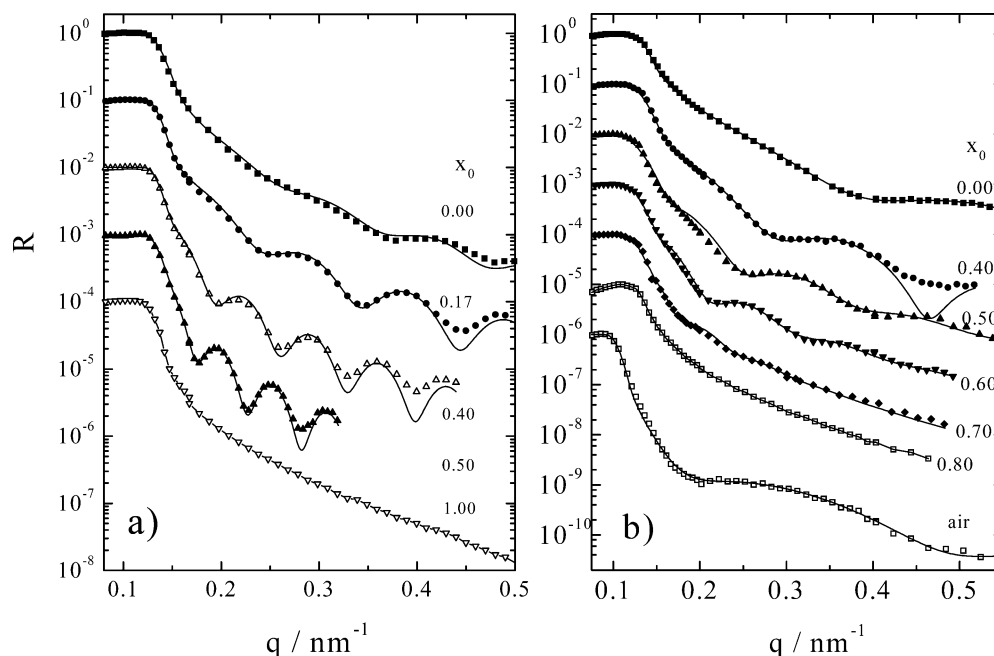
Already in the original $R(q)$ -data the swelling of the brush with increasing toluene content in the solvent is obvious from the narrowing of the Kiessig fringes. The thicknesses obtained for the collapsed layer in methanol agrees very well with the X-ray reference data as well as with a NR scan taken in air. The addition of only 17 vol.%, corresponding to 7 mol% of toluene to methanol causes the brush to swell by ca. 10% as can be clearly deduced from the enhanced spatial frequency in the Kiessig fringes and their Fresnel fit curve. Upon

Table 1 Parameters used for the simulations of the X-ray reflectivity data (cf. Fig. 2) from the dry PS samples obtained by a Fresnel algorithm

Dry PS thickness d_0/nm	Electron density $a\rho_e$ (Si) ^(a) / $10^3 \text{ e} \cdot \text{nm}^{-2}$	Electron density $a\rho_e$ (PS) ^(a) / $10^3 \text{ e} \cdot \text{nm}^{-2}$	Interfacial roughness $\sigma_{\text{Si/PS}}/\text{nm}$	Interfacial roughness $\sigma_{\text{PS/air}}/\text{nm}$
19.5	18.92	9.67	1.8	0.65
53.0	20.48	9.65	1.1	0.60

^a $a = 2.82 \times 10^{-15} \text{ m}$ is the classical electron radius

Fig. 3a,b Neutron reflectivity curves, R -vs- q , for polystyrene brushes with a dry thickness of: **a** $d_0 = 53$ nm; **b** $d_0 = 19.5$ nm but swollen in solvent mixtures of per-deuterated methanol and per-deuterated toluene of different volume fractions, x_0 , of toluene. Symbols are the data points, the full curves are Fresnel fits based on the scattering length density profiles, $\frac{b}{V}$, given in Fig. 4. Same samples as in Fig. 2



further increase of the toluene content the brush swells further with the Kiessig fringes being even more pronounced. However, only up to a certain limit: the NR data taken in 80 vol.% toluene show no obvious Kiessig modulation anymore, and hence the whole profile analysis has to be limited to the range $0 \leq x_0 \leq 0.70$. This means, in particular, that we cannot follow the swelling of the brush up to toluene contents in the mixed solvent that would correspond to the Θ -mixture for free PS-chains which is reported as $x_0 = 0.80$ [26, 27].

We should emphasize that, based on the fit to the reliable data range from $R=1$ to about $R \approx 10^{-3}$, the experimental results gave us no reason to describe the brushes other than by a box model with a limited interfacial smearing of the brush/solvent interface. The assumption of a flat scattering length density profile and the mentioned Gaussian rounded step profile was enough to obtain satisfying agreement between the fit calculations and the experimental data. No other detail had to be added to the profile. Even when trying to force the fit to include a more extended feature like an exponential tail [18] for the polymer density profile, the $1/e$ decay length of this tail for the thicker sample was in no case larger than 2.5 nm. This means that in any simulated curve compatible with our data the width of the interface brush/solvent amounts to less than 20% of the total layer thickness which otherwise exhibits a constant density profile. This means that also no other fancy feature like a wetting polymer layer on top of the compressed brush or any excess polymer near the SiO_2 surface [15] could be seen in our data.

This interpretation would need to be somewhat modified if the deviations between the fit curve and the

data at high momentum transfer, i.e., at reflectivities in the $R = 10^{-4}$ range, were to be taken seriously. We exemplify this for the curve taken with the thinner sample at 40 vol.% toluene. Figure 5a shows an improved agreement between the experimental data at high q and the calculated curve which could be modeled by assuming a modified scattering length density profile of the brush, near the brush/solvent interface. The best-fit profile is displayed in Fig. 5b, together with the “smeared-box” profile displayed already in Fig. 4b.

Two conclusions can be drawn from this comparison. (1) In order to be able to deduce subtleties of the detailed brush profile, NR data have to be taken also at substantially higher momentum transfer, i.e., however, at largely reduced intensities. (2) These details have no (major) consequence on the accuracy of the thickness and the average scattering length density profile of the swollen brush and hence do not interfere significantly with our conclusions.

The finding of a constant scattering length density profile is in excellent agreement with the theoretical expectations for dense brushes where the blob model predicts a flat chain segment density across the brush [5]. The predicted depletion for noninteracting grafted polymers near the solid surface scales with the chain separation distance D which for our samples were in the range of 3 to 5 nm. This effect could, therefore, not be resolved by our reflectivity measurements. Experimentally, the smearing of the chain ends in contact to the solvent is certainly broadened compared to the theoretical predictions because of the polydispersity which is unavoidable by this polymerization procedure. However, as we could show by independent investigations,

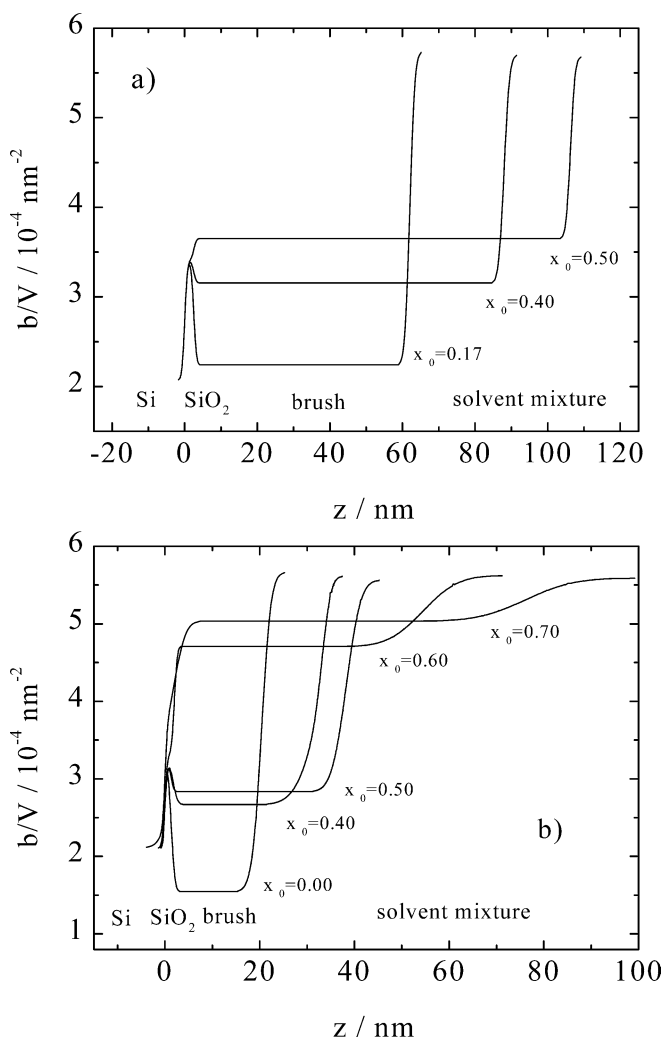


Fig. 4a,b Scattering length density profiles, $\frac{b}{V}$ -vs- z , as obtained from the neutron reflectivity curves given in Fig. 3 obtained: **a** from the sample with a dry thickness of $d_0 = 53$ nm; **b** from the one with $d_0 = 19.5$ nm. x_0 denotes the volume content of toluene in the solvent mixture with methanol

the “grafting-from” scheme results in similar molecular weight distributions as for the corresponding free radical polymerization in bulk solution. The obtained polydispersity in the range of $\overline{M}_w/\overline{M}_n = 1.5$ – 2.5 does not significantly interfere with the chain stretching phenomenon of dense brushes.

The layer thickness increase with increasing toluene content, x_0 , in the solvent mixture is given in Fig. 6a. Plotted are the thicknesses d_B as obtained from the scattering length density profiles presented in Fig. 4a,b scaled to the dry collapsed thickness d_0 . Shown is the swelling behavior of three different samples with different thicknesses. The maximum thickness increase that can be identified in the Kiessig fringes amounts to a factor of 3.7. The experimental data are also summa-

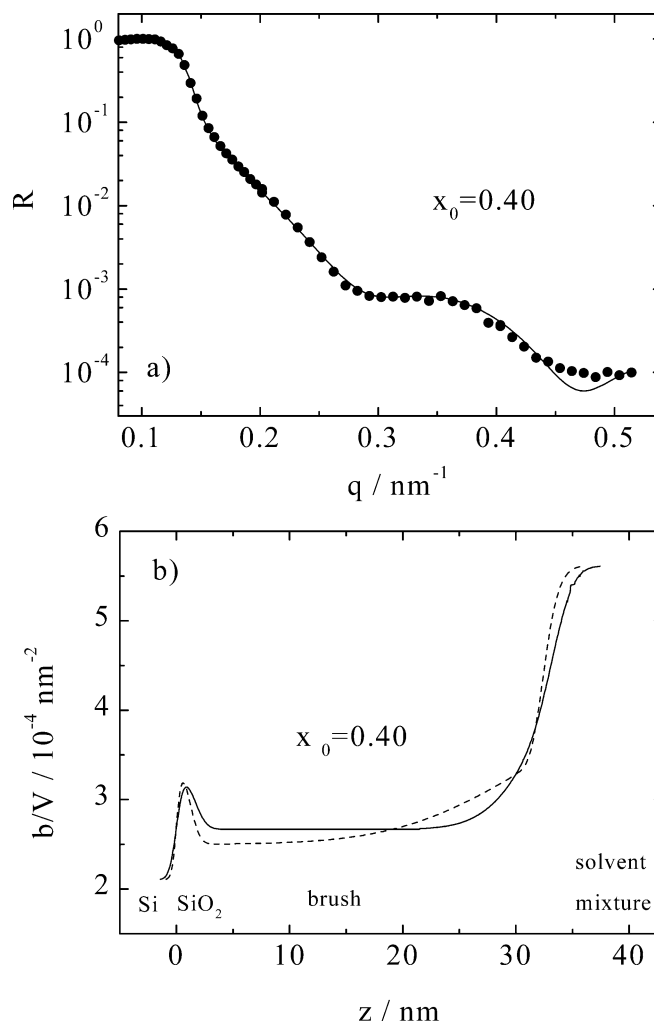


Fig. 5a,b Refinement of the scattering length density profile for the thin sample ($d_0 = 19.5$ nm) in a solvent mixture containing toluene at a volume fraction of $x_0 = 0.40$: **a** reflectivity data reproduced from Fig. 3b. The *full curve* is a Fresnel fit based on a refined profile given in **b**, *dashed line*. For comparison, the profile from Fig. 4b is reproduced. Note, that the fit describes the reflectivity data at high q , i.e., at low reflectivities ($R \approx 10^{-4}$) better, but the mean scattering length density in the brush, as well as its thickness are not significantly changed

ri- zed in Table 2 for sample 1, and in Table 3 for sample 3, respectively.

The increase in the scattering length density of the swollen brush which is the result of the up-take of the deuterated solvent molecules is given in Fig. 6b. Shown are the data points derived from the profiles given in Fig. 4a,b (cf. also Tables 2 and 3, respectively). The solid curve corresponds to the expectation based on the thickness increase: Ignoring possible changes of the apparent partial molar volumes of toluene and methanol in a mixture with grafted polystyrene (which was determined for free PS chains of $\overline{M}_n = 190,000$ g/mol to be $\Delta V_M = -4.12$ cm³/mol corresponding to ca. 5%) [28]

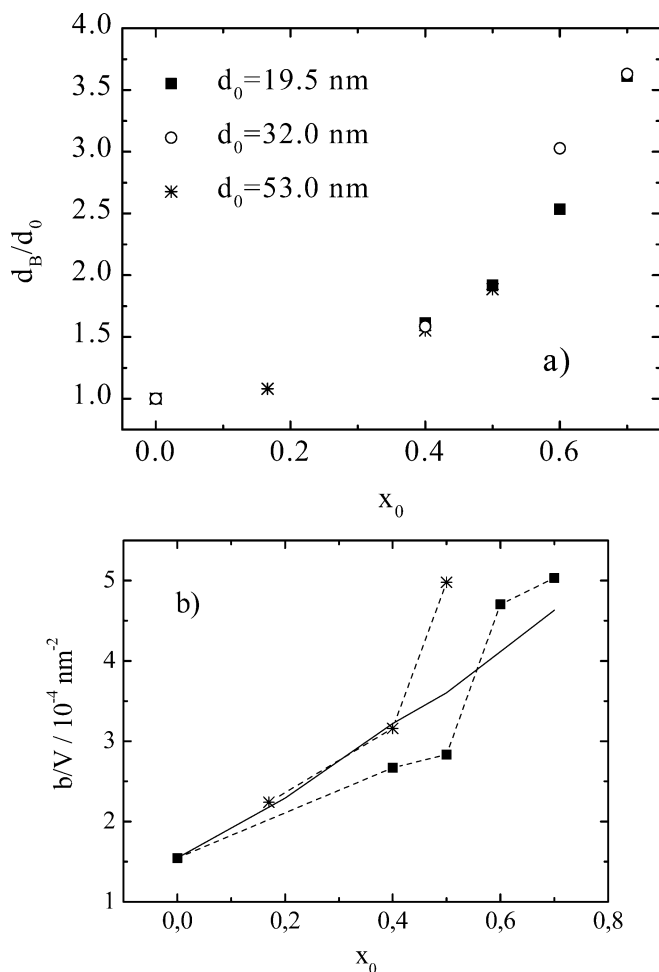


Fig. 6a,b Swelling behavior of polystyrene brushes of different initial (dry) thickness d_0 as obtained from the scattering length density profiles given in Fig. 4: **a** the thickness values of the brush, d_B , scaled to their dry thickness, d_0 , as a function of the volume fraction, x_0 , of toluene in the solvent mixture; **b** the corresponding plateau values of the scattering length density of the swollen brush; symbols are as in a. The full line gives the expected increase in the scattering length density based on the thickness increase (for details, see text)

Table 2 Scattering length densities, $\frac{b}{V}$, for methanol/toluene solvent mixtures of different toluene volume fractions, x_0 , and the obtained thicknesses and scattering length densities of the sample with a dry thickness of $d_0 = 53$ nm after swelling in these solvent mixtures

Solvent			Brush ($d_0 = 53$ nm)	
Volume fraction	Mole fraction	$\frac{b}{V} _{\text{solvent}} / 10^{-4} \cdot \text{nm}^{-2}$	Thickness d_B/nm	$\frac{b}{V} _{\text{Brush}} / 10^{-4} \cdot \text{nm}^{-2}$ ($\pm 0.1 \cdot 10^{-4} \text{nm}^{-2}$)
x_0	x_{mole}			
0.17	0.07	5.74	59.5	2.2
0.40	0.20	5.69	85.5	3.2
0.50	0.27	5.68	103.8	3.7
1.0	1.0	5.58	350.0	5.0

Table 3 Scattering length densities, $\frac{b}{V}$, for methanol/toluene solvent mixtures of different toluene volume fractions, x_0 , and the obtained thicknesses and scattering length densities of the sample with a dry thickness of $d_0 = 19.5$ nm after swelling in these solvent mixtures

Solvent			Brush ($d_0 = 19.5$ nm)	
Volume fraction	Mole fraction	$\frac{b}{V} _{\text{solvent}} / 10^{-4} \cdot \text{nm}^{-2}$	Thickness d_B/nm	$\frac{b}{V} _{\text{Brush}} / 10^{-4} \cdot \text{nm}^{-2}$ ($\pm 0.1 \cdot 10^{-4} \text{nm}^{-2}$)
x_0	x_{mole}			
0	0	5.78	19.5	1.6
0.40	0.20	5.72	31.5	2.5
0.50	0.27	5.71	37.4	2.7
0.60	0.36	5.70	49.4	4.7
0.70	0.47	5.68	75.1	5.0
0.80	0.60	5.67	≈ 90.1	5.2

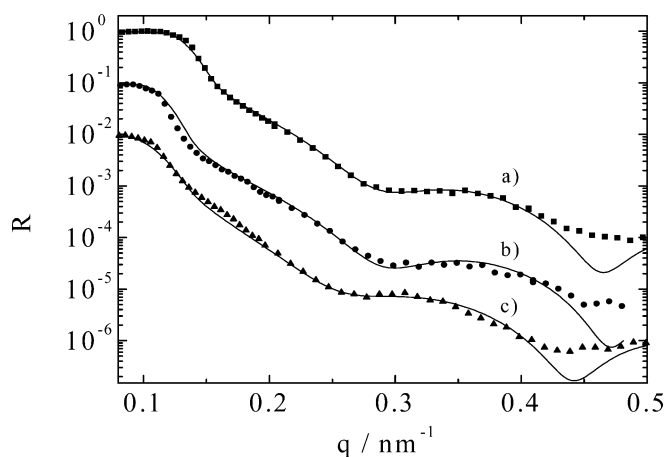


Fig. 7 Contrast variation experiments with the brush of $d_0 = 19.5$ nm in a methanol/toluene mixture of $x_0 = 0.40$. Curve a) was taken with both components of the mixture in fully deuterated form (reproduced from Fig. 3b). Curve b) was taken also with a solvent mixture of $x_0 = 0.40$, however, one-third of the methanol was protonated. Curve c) was again recorded with $x_0 = 0.40$, but half of the toluene was used in the protonated form. Symbols are the data points, the full curves are Fresnel fits that yield virtually the same thickness but different plateau values of the scattering length density in the brush from which the composition of the solvent mixture in the brush can be deduced

we can describe the scattering length density of the swollen film as the sum of two contributions, i.e., polystyrene and solvent, according to their respective volume fraction, i.e.,

$$\frac{b}{V}|_{\text{Brush}} = \frac{b}{V}|_{\text{PS}} \frac{d_0}{d} + \frac{b}{V}|_{\text{Solvent}} \cdot \frac{(d - d_0)}{d} \quad (1)$$

The experimentally determined scattering length densities of the swollen brushes, $\frac{b}{V}|_{\text{Brush}}$, show qualitatively the behavior expected from the thickness increase. However, this analogy only holds because the scattering length densities of perdeuterated toluene and methanol are almost identical. That means that $\frac{b}{V}|_{\text{Solvent}}$ can be

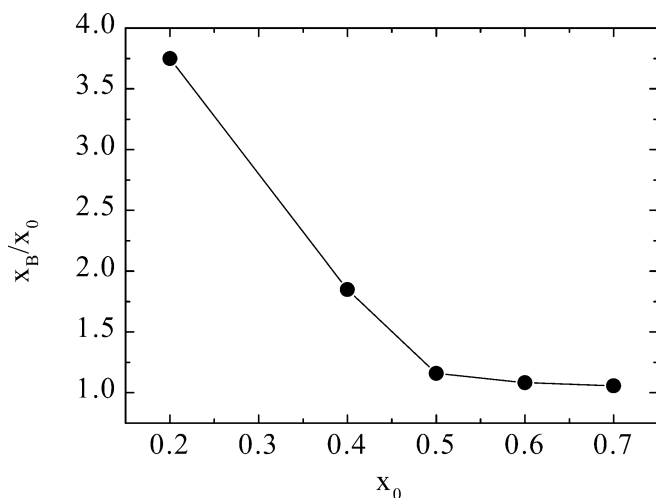


Fig. 8 Preferential incorporation of toluene into the swollen brushes: given are the volume fractions, x_B , of toluene in the brushes, scaled to the fraction in the bulk mixture, x_0 , as a function of x_0

(approximately) calculated, irrespective of any preferential incorporation of one of the components of the solvent mixture.

In order to determine such a possible preferential solvation we performed contrast variation experiments,

i.e., swelling experiments at a fixed mole fraction x_0 of toluene but with different ratios of protonated and deuterated solvents. Figure 7 displays three reflectivity curves that were taken in three different solvent contrasts. Figure 7a is reproduced from Fig. 3b and shows the curve measured in the per-deuterated solvent mixture. Figure 7b was obtained from a mixture with identical toluene content, but one-third of the methanol was used in the protonated form, whereas the curve in Fig. 7c was measured with half of the toluene being protonated. From the obtained scattering length density variations of the swollen brushes one can determine the mole fraction x_B of the solvent mixture in the brush as a function of the mole fraction x_0 of the bulk solvent mixture. The result for all investigated mixtures is given in Fig. 8. One can see that, indeed, for the mixtures with a low content of toluene, $x_0 < 0.50$, a strong preference for the incorporation of toluene, i.e., the good solvent, into the brush can be seen. These findings confirm quantitatively earlier qualitative observations of a preferential solvation of grafted PS by toluene [19]. We should point out, however, that this analysis is based on the assumption that the brush segment density profile parallels the solvent (composition) profile. This does not need to be the case, necessarily! A more detailed analysis along these lines is in progress.

References

- Milner ST (1991) *Science* 251:905
- Halperin A, Tirrell M, Lodge TP (1992) *Adv Polym Sci* 100:31
- Halperin A (1994) In: Rabin Y, Bruinsma R (eds) *Soft order in physical sciences*. Plenum Press, New York, p 33
- Alexander S (1977) *J Phys (Paris)* 38:983
- de Gennes PG (1980) *Macromolecules* 13:1069
- Milner ST, Witten TA, Cates ME (1988) *Macromolecules* 21:2610
- Shim DFK, Cates ME (1989) *J Phys France* 50:3535
- Zhulina EB, Borisov OV, Pryamitsyn VA, Birshtein TM (1991) *Macromolecules* 24:140
- Lai PY, Binder K (1992) *J Chem Phys* 97:586
- Grest GS, Murat M (1993) *Macromolecules* 26:3108
- Whitmore MD, Noolandi J (1990) *Macromolecules* 23:3321
- Doyle PS, Shaqfeh ESG, Gast AP (1997) *Phys Rev Lett* 78:1182
- Field JB, Toprakcioglu C, Ball RC, Stanley HB, Dai L, Barford W, Penfold J, Smith G, Hamilton W (1992) *Macromolecules* 25:434
- Kumachev E, Klein J, Pincus P, Fetters LJ (1993) *Macromolecules* 26:6477
- Perahia D, Wiesler DG, Satija SK, Fetters LJ, Sinha SK, Milner ST (1994) *Phys Rev Lett* 72:100
- Lin Y, Quinn J, Rafailovich MH, Sokolov J (1995) *Macromolecules* 28:6347
- Mansfield TL, Iyengar DR, Beaucage G, McCarthy TJ, Stein RS, Composto RJ (1995) *Macromolecules* 28:492
- Karim A, Satija SK, Douglas JF, Anker JF, Fetters LJ (1994) *Phys. Rev Lett* 73:3407
- Auroy P, Auvray L (1992) *Macromolecules* 25:4134
- Auroy P, Auvray L, Leger L (1991) *Phys Rev Lett* 66:719
- Prucker O, Rhe J (1998) *Macromolecules* 31:592
- Foster M, Stamm M, Reiter G, Httenbach S (1990) *Vacuum* 41:1441
- Stamm M (1992) In: Sanchez IC, Fitzpatrick LE (eds) *Physics of polymer surfaces and interfaces*. Butterworth-Heinemann, Boston London Oxford, p 163
- Lekner J (1987) *Theory of reflection*. Martinus Nijhoff, Dordrecht Boston Lancaster
- Stamm M, Httenbach S, Reiter G (1991) *Physica B* 173:11
- Brandrup J, Immergut EH (eds) (1989) *Polymer handbook*, 3rd edn. Wiley, New York, chap 5, p 82
- Oth J, Desreux V (1954) *Bull Soc Chim Belg* 63:285
- Bianchi U, Cuniberti C, Pedemonte E, Rossi C (1969) *J Polym Sci* 7:855